processes

MDPI

Article

Effect of Acid Fluid on Deep Eocene Sweet Spot Reservoir of Steep Slope Zone in Lufeng Sag, Pearl River Mouth Basin, South China Sea

Kai Zhong [1,2], Lihao Bian [1,2,*], Shijie Zhao [1,2] and Kailong Feng [1,2]

[1] State Key Laboratory of Marine Geology, Tongji University, No. 1239 Siping Road, Shanghai 200092, China; zhongkai@tongji.edu.cn (K.Z.); zhaoshijie9267@163.com (S.Z.); fengkailong@tongji.edu.cn (K.F.)
[2] Center for Marine Resources, Tongji University, No. 1239 Siping Road, Shanghai 200092, China
* Correspondence: 2210844@tongji.edu.cn

Abstract: The Paleogene system of the Zhuyi Depression exhibits a pronounced mechanical compaction background. Despite this compaction, remarkable secondary porosity is observed in deep clastic rocks due to dissolution processes, with well-developed hydrocarbon reservoirs persisting in deeper strata. We conducted a comprehensive study utilising various analytical techniques to gain insights into the dissolution and transformation mechanisms of deep clastic rock reservoirs in the steep slope zone of the Lufeng Sag. The study encompassed the collection and analysis of the rock thin sections, XRD whole-rock mineralogy, and petrophysical properties from seven wells drilled into the Eocene. Our findings reveal that the nature of the parent rock, tuffaceous content, dominant sedimentary facies, and the thickness of individual sand bodies are crucial factors that influence the development of high-quality reservoirs under intense compaction conditions. Moreover, the sustained modification and efficient expulsion of organic–inorganic acidic fluids play a main role in forming secondary dissolution porosity zones within the En-4 Member of the LF X transition zone. Notably, it has been established that the front edge of the fan delta, the front of the thin layer, and the near margin of the thick layer of the braided river delta represent favorable zones for developing deep sweet-spot reservoirs. Furthermore, we have identified the LF X and LF Y areas as favourable exploration zones and established an Eocene petroleum-accumulation model. These insights will significantly aid in predicting high-quality dissolution reservoirs and facilitate deep oil and gas exploration efforts in the steep slope zone of the Zhuyi Depression.

Keywords: fault basin; Eocene; deep acid fluids; secondary porosity; high quality reservoirs

Citation: Zhong, K.; Bian, L.; Zhao, S.; Feng, K. Effect of Acid Fluid on Deep Eocene Sweet Spot Reservoir of Steep Slope Zone in Lufeng Sag, Pearl River Mouth Basin, South China Sea. *Processes* **2024**, *12*, 895. https://doi.org/10.3390/pr12050895

Academic Editors: Zheng Sun, Dongya Zhu, Kun He, Jia Wu and Qingqiang Meng

Received: 26 February 2024
Revised: 25 April 2024
Accepted: 25 April 2024
Published: 28 April 2024

1. Introduction

The deep-ultra-deep reservoirs represent one of the most important frontiers in global oil and gas exploration [1–3]. However, a clear understanding of the primary controlling factors for developing high-quality reservoirs remains elusive, limiting further exploration. Therefore, in deep and ultra-deep basins with low permeability and tight environments, the discovery of high-quality sandstone reservoirs resulting from secondary porosity related to dissolution with better petrophysical properties is the key to successful exploration [4–8]. Recent explorations in deep-ultra-deep strata of various oil-bearing basins have yielded significant findings. Notably, high-quality clastic rock reservoirs have been discovered at depths of 4800 m in the Beihai Graben [9], 6000 m in the Gulf of Mexico Basin [4], 4000 m in the Zhanhua Depression of the Bohai Bay Basin [10], and even 7000 m in the Tarim Basin [11]. These discoveries highlight the potential for high-quality reservoirs in deep-ultra-deep strata and underscore the need for a deeper understanding of the controlling factors that shape their development.

The Pearl River Mouth Basin has been identified as harbouring several hydrocarbon-rich depressions. Among them, the Zhuyi Depression, situated in the northern region of the Pearl River Mouth Basin, has garnered significant attention from researchers due to its rich oil-bearing potential [12,13]. Previous studies have offered valuable insights into the basin's structure, fault system, fault activity, and tectonic evolution [14–18]. As the exploration process has deepened, the Lufeng Sag, the secondary structural unit of the Zhuyi Depression, has emerged as a prime focus, particularly in the deep Eocene strata. What is more, the organic–inorganic interaction of acidic fluid produced during the maturation of organic matter can promote dissolution development [19,20]. This area has confirmed several commercial and potentially commercial discoveries, making it the most actively explored Paleogene region within the Pearl River Mouth Basin [21]. Oil and gas discovery in the Lufeng Sag are primarily concentrated in the gentle slope zone, far away from the depression control fault. However, it is noteworthy that the steep slope zone, being proximal to the controlling faults of the depression, holds immense potential for untapped oil and gas resources. In addition, drilling has confirmed the presence of large fan deltas in the steep slope zone, indicating favourable geological conditions for hydrocarbon accumulation. Despite this, the complexity of reservoir development and oil–gas accumulation mechanisms has limited the exploration efforts in this region. Wang et al. conducted a comprehensive analysis of the primary controlling factors influencing reservoir formation, considering factors such as sedimentation, diagenesis, and early tectonic uplift [22]. Zhu et al. extended this understanding by examining the protective role of oil and gas charging on reservoir quality, building upon sedimentary and diagenetic studies [23]. The previous research on the Lufeng Sag, despite its extensive exploration of deep high-quality reservoirs, has notably overlooked an analysis of the sweet-spot reservoir scale in the steep slope zone. This study addresses this gap by employing various analytical techniques, including rock-thin section analysis, XRD whole-rock-mineral analysis, and rock petrophysical-property tests. The objective is to comprehensively understand the reservoir characteristics in the deep steep slope zone and clarify the effect of deep acid fluid transformation on the formation mechanism and distribution mode of high-quality reservoirs. Using logging and seismic analysis, fluid-inclusion analysis, and fault-activity analysis, a favourable reservoir-forming area in the steep slope belt of Lufeng Sag is predicted, and the reservoir-forming model is established. This is very important for deep oil and gas exploration in the steep slope zone of Lufeng Sag and can also provide the direction for the next steep slope belt oil and gas exploration in other hydrocarbon-rich depressions in the Zhuyi Depression.

2. Geological Setting

The Pearl River Mouth Basin is a Cenozoic oil-bearing basin located on the northern shelf of the South China Sea. The basin was formed based on the extensional fault depression beginning at the end of the Mesozoic era, with an NE–SW distribution. The basin can be divided into five first-order tectonic units, including the northern uplift belt, the northern depression belt (Zhuyi and Zhusan depressions), the central uplift belt, the southern depression belt (Zhuer depression), and the southern uplift belt (Figure 1) from north to south [12,23–25]. Lufeng Sag is located northeast of the Zhuyi Depression, with an area of 7760 km^2. It is bordered by the North Uplift Zone to the north, the Hanjiang Sag to the east, the Dongsha Uplift to the south, and the Huizhou Sag to the west [19,26–28].

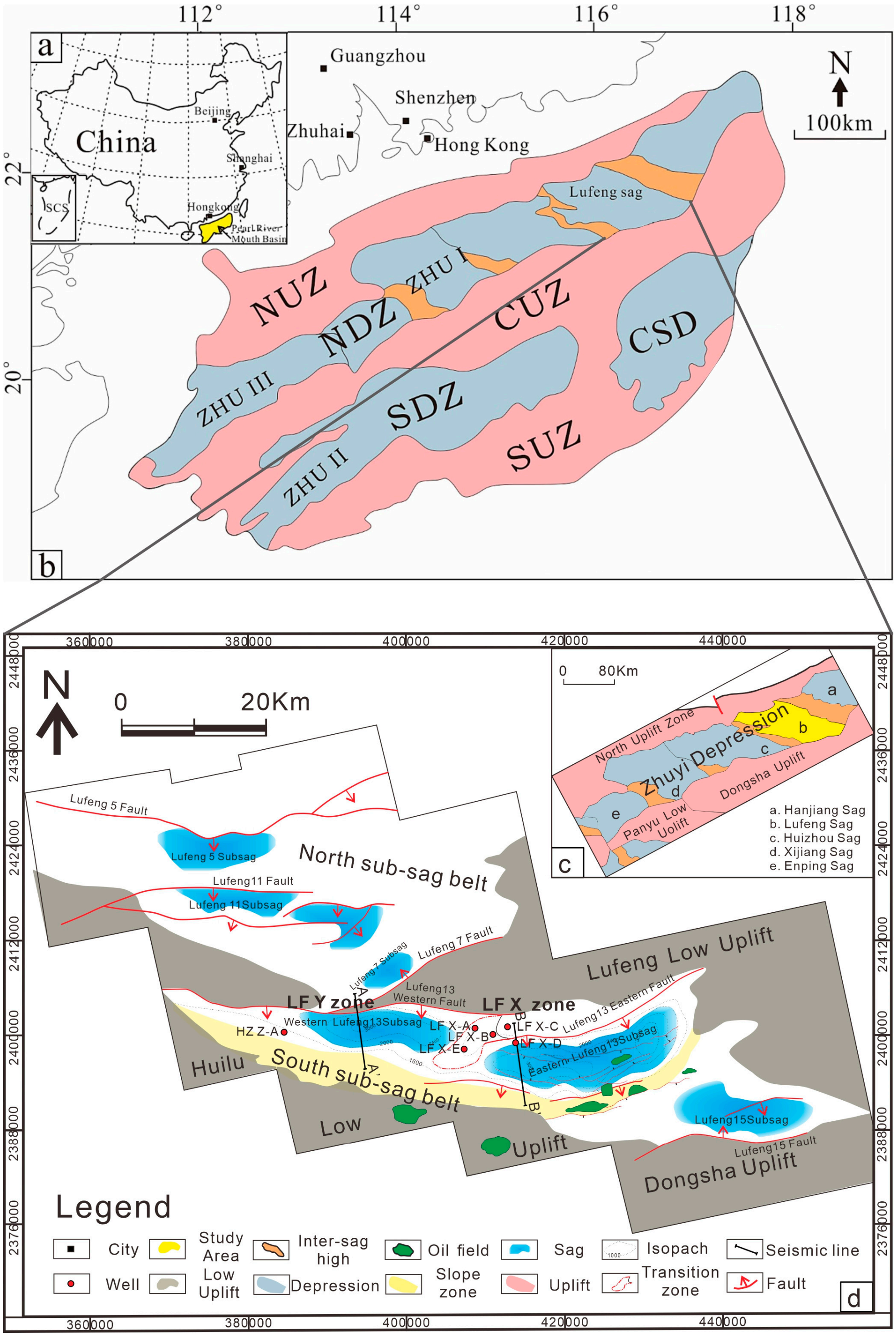

Figure 1. Structural unit division of Lufeng Sag, Pearl River Mouth Basin, (**a**) Location of the Pearl River Mouth Basin in the South China Sea. (**b**) Cenozoic structural units of the Pearl River Mouth Basin, and the location of Lufeng Sag, SCS: South China Sea, ZHU I: Zhuyi Depression, ZHU II: Zhuer Depression, ZHU III: Zhusan Depression, NUZ: Northern Uplift Zone, CUZ: Central Uplift Zone, SUZ: Southern Uplift Zone, SDZ: Southern Depression Zone, NDZ: Northern Depression Zone, CSD: ChaoShan Depression. (**c**) Internal structural unit of Zhuyi depression; (**d**) Structural unit, key well, and survey line location in the study area (Modify from Wang et.al., 2022 [3]).

The Lufeng Sag experienced six major tectonic movements during the Cenozoic: the first episode of the Zhuqiong movement, the Huizhou movement, the second episode of the Zhuqiong movement, the South China Sea movement, the Baiyun movement, and the Dongsha movement. The first episode of the Zhuqiong movement triggered the commencement of faulting activities, during which the Lower Wenchang Formation was deposited in the research area. It was primarily composed of semi-deep lacustrine-to-deep lacustrine mudstones, which is conducive to the formation of high-quality source rock. Following the Huizhou movement, the faulting activities subsided, leading to the deposition of the Upper Wenchang Formation, which was primarily characterized by shallow lacustrine facies. After the second episode of the Zhuqiong movement, the faulting activities intensified, resulting in the deposition of the Enping Formation. The Lower Enping Formation is mainly composed of deep lacustrine deposits, while the Upper Enping Formation is dominated by braided river deposits. In addition, the steep slope zone continued to develop a fan delta close to the depression control fault during this period, which made the fault become an important channel between the source rock of the Lower Wenchang Formation and the fan delta (Figure 2). From the depositional period of the Wenchang Formation to the Enping Formation, the extensional direction of the basin experienced a shift from NW–SE to N–S [29–34]. The South China Sea movement responds to seafloor spreading in the continental margin. The evolution of the northern continental margin basin has since entered the intercontinental rift-passive continental margin stage, and the subsidence mechanism of the basin is affected by thermal subsidence (Figure 2). On the basis of the Mesozoic fold basement, the Lufeng Sag deposited stratum from Paleogene to Quaternary and includes Wenchang and Enping formations in the faulting period, Zhuhai, Zhujiang and Hanjiang formations in the thermal subsidence period, and Yuehai and Wanshan formations in the Neotectonic period [14,15]. This study focuses on the Wenchang and Enping Formation of Eocene. The Wenchang Formation can be divided into six members, of which the Wen-6, Wen-5, and Wen-4 members deposited after the first episode of the Zhuqiong movement formed the Xiawenchang Formation, and the Wen-3, Wen-2, and Wen-1 members deposited after the Huizhou movement formed the Upper Wenchang Formation. The Enping Formation is mainly deposited after the second episode of the Zhuqiong movement and can be divided into the Lower Enping Formation composed of En-4 and En-3 members and the Upper Enping formation composed of En-2 and En-1 members.

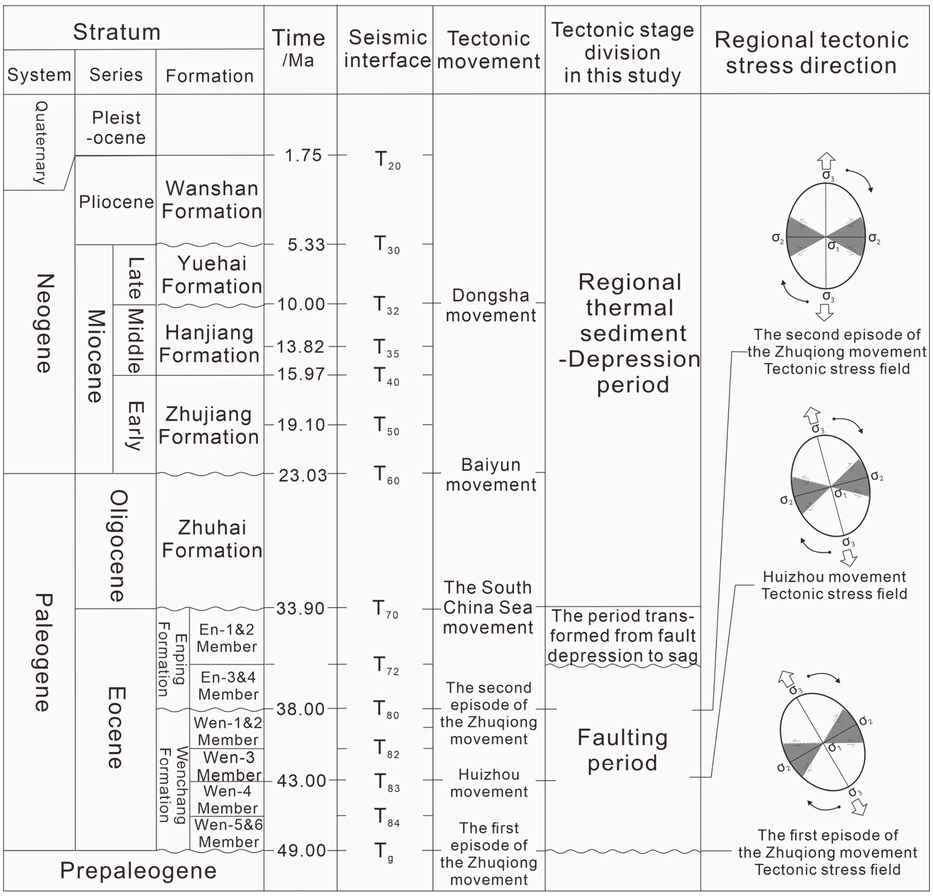

Figure 2. Structure-stratigraphic framework of Lufeng Sag, Pearl River Mouth Basin.

3. Data and Methods

3.1. Data and Samples

In this study, the sample of core or cuttings was collected from 23 wells in the steep slope zone of Lufeng Sag at 57 depth points in the Eocene, and 1140 thin sections were obtained using polarizing microscope with plane polarized light and perpendicular polarized light for petrological and petrographic analysis of cast thin sections, and we mainly introduce the thin section analysis of six typical wells in this paper. In addition, we also collected critical reservoir test data such as XRD whole-rock-mineral analysis, XRF analysis, and rock petrophysical-property-test analysis of six wells, as well as crucial reservoir formation data such as fluid inclusion data of two wells from the cooperating oil companies.

3.2. Methods

The combined logging-seismic-thin section analysis is an essential method in reservoir research. The purpose is to characterize the reservoir structure and analyze its internal distribution characteristics with the help of drilling data with high vertical resolution, seismic data with high lateral resolution, and delicate microscopic thin section data to form a complete and accurate reservoir-analysis method. The 3D seismic analysis in the study area is mainly based on Petrel software (Version 2018), which mainly includes the identification and characterization of Eocene's fan delta and braided river delta and the fault activity analysis during reservoir formation. The logging data are mainly processed by Resform software (Version 3.5), which researches the essential petrophysical characteristics of different intervals and high-quality reservoir analysis. In addition, all of the critical reservoir test data and fluid inclusion data were collected from the cooperating oil companies. Rock petrophysical properties are measured by helium-porosity-measuring instrument and Core Measurement System (CMS)—300 equipment. XRD whole-rock-mineral analysis is conducted to obtain the mineral composition of the sample and obtain the lithology of the test sample according to the mineral combination. The research method of fluid inclusions is mainly to determine the reservoir formation information of oil and gas from generation to migration to accumulation by obtaining its uniform temperature data and combining it with the evolution of tectonic movement.

4. Results

4.1. Characteristics of Eocene Reservoir in Steep Slope Zone of Lufeng Sag

In this study, the thin-section analysis shows that the clastic components of the reservoir in the steep slope zone of Lufeng Sag are mainly quartz, followed by rock debris, and the content of feldspar is low. In addition, the sandstones are mainly medium sand, followed by coarse sand, fine sand, and conglomerate. The sorting is medium-poor, the roundness is mainly sub-angular and sub-roundness, some particles have good roundness, and the contact between particles is mainly linear. The high mud content may result in poor petrophysical properties in the Enping Formation (Figure 3).

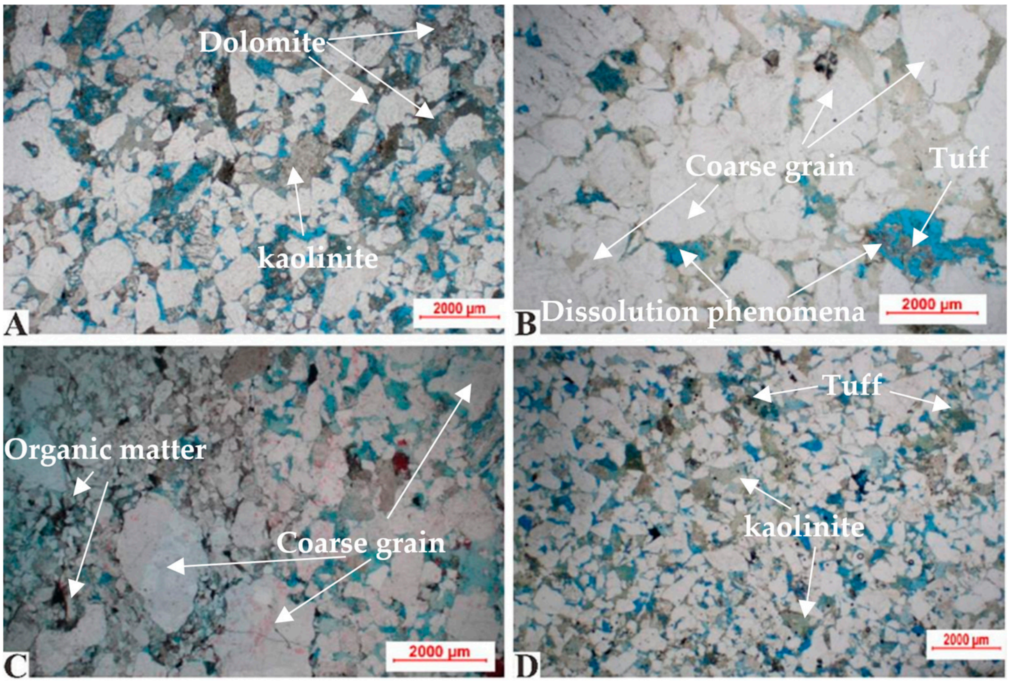

Figure 3. The typical thin-section photos of sandstone reservoir in steep slope zone of Lufeng Sag: (**A**) Well LF X-A, 3776.8 m, En-4 member, mainly sandstone with a small amount of dolomite and clay minerals, and the clastic particles are poorly sorted, mainly medium, coarse, and giant particles, and a small amount of gravel. The intergranular pores are well developed; (**B**) Well LF X-B, 3883 m, Prepaleogene, the clastic particles are mainly coarse and some gravel, with dissolution phenomena and a large amount of tuff, poor pore development, and poor connectivity; (**C**) Well LF X-C, En-3 Member, 3596 m, is mainly composed of sand and kaolinite, poor sorting, mainly coarse grain, followed by medium grain, a few gravel and fine grain; the pores are mainly secondary pores developed, the overall pores are poorly developed, and some organic matter remains; (**D**) Well LF X-D, 3569 m, En-3 member, mainly coarse grain, partly medium grain, and a small amount of tuffaceous matter, with noticeable authigenic kaolinite pores.

The sandstone reservoir in the study area is dominated by interparticle pores, accounting for 34% of all pores, followed by intercrystal pores and intra-granular dissolved pores (Figure 4). In addition, the secondary intergranular dissolution pores, intra-granular dissolution pores, and mold holes also occupy a relatively large scale. The three are related to dissolution, accounting for 38.3% of the total, indicating that the sandstone reservoir in the steep slope zone of Lufeng Sag still has a strong dissolution effect to increase the scale of pores. Therefore, it is very important to identify the main zones and controlling conditions of dissolution development for searching the high-quality deep sandstone reservoir under the background of strong compaction.

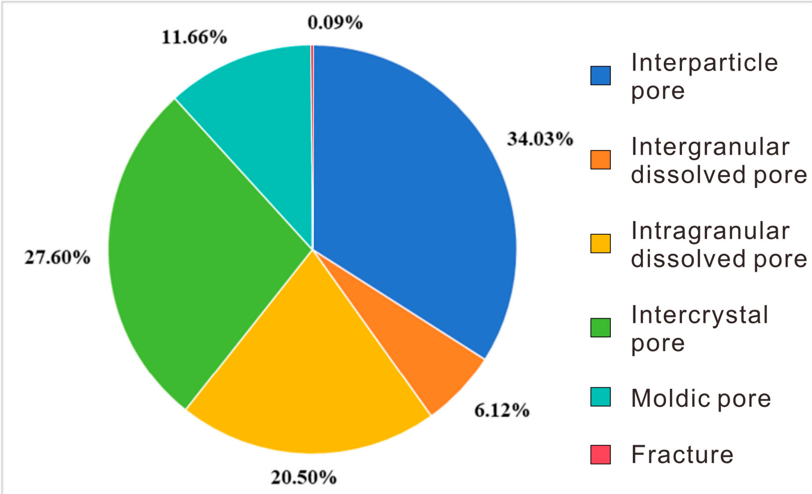

Figure 4. Pie chart of pore proportion of the Wenchang-Enping Formation in steep slope zone of Lufeng Sag, and various types of pores are shown in the following thin section photos.

In addition, by analyzing the pore type development and distribution characteristics between the different menbers, it can be clear that there may be secondary dissolution pore development zones in the En-4, Wen-5 and Wen-4 Members of the deep sandstone reservoir. In the non-dissolution pore types, the proportion of residual interparticle pores of the Wenchang–Enping Formation significantly increased upward in two cycles, indicating that both cycles were affected by mechanical solid compaction (Table 1). Among the pore types caused by dissolution,, Wen-5 and 6 members have the highest proportion of intragranular dissolved pores, and Wen-5 and 6 and En-4 members have the highest proportion of dissolved pores (except for Wen-1 and 2 members), which gradually decreases upward, indicating that dissolution is the most influential factor for increasing pores in the Lower Wenchang Formation under the strong compaction (Table 1).

Table 1. Distribution characteristics of pore types of sandstone reservoirs of Wenchang-Enping Formation in the steep slope zone of Lufeng Sag.

Stratum	Areal Porosity (%)							
	Interparticle Pore	**Intergranular Dissolved Pore**	**Intragranular Dissolved Pore**	**Intercrystal Pore**	**Moldic Pore**	**Fracture**	**Total Dissolved Pore**	**Total Pore**
Wen-5 and 6 Member	2.21	0	1.14	2.14	1.36	0.07	4.64	6.92
Wen-4 Member	4.78	0	0.75	1.7	0.9	0	3.35	8.13
Wen-3 Member	7.5	0	0.25	0.5	1	0	1.75	9.25
Wen-1 and 2 Member	0	0	4	0	3	0	7	7
En-4 Member	1.96	0.27	1.19	2.42	1.27	0	5.15	7.11
En-3 Member	2.56	1.08	1.33	2.34	0.13	0	4.88	7.44
En-1 and 2 Member	3.82	0.31	0.93	2.06	0.25	0	3.55	7.37

4.2. The Influence of Diagenesis on Reservoir Petrophysical Properties

Through the analysis of 1140 thin sections from 57 depth points, five types of diagenesis, namely mechanical compaction, calcareous cementation, argillous cementation, carbonate cementation, and dissolution, are identified in Lufeng Sag.

The Wenchang–Enping Formation sandstone reservoir in the steep slope zone of Lufeng Sag has generally experienced strong compaction. Under the influence of strong compression, the overall porosity of the reservoir decreases with the increase of buried depth (Table 1). With the increase of buried depth, the porosity of the Wenchang Formation reservoir decreases significantly, the permeability decreases, and the petrophysical property deteriorates. The effect of compaction on the sandstone reservoir of the Enping Formation is significantly reduced compared with the Wenchang Formation. Compaction is a crucial factor, leading to poor reservoir petrophysical properties in the study area. This process causes tight contacts and compression fractures between mineral particles, deformation of plastic minerals, and pseudo-matrix of feldspar and rock debris, which restrict pore space and fluid flow, decreasing reservoir porosity and permeability (Figure 5). Overall, compaction adversely affects reservoir quality, challenging the region's effective oil and gas exploration.

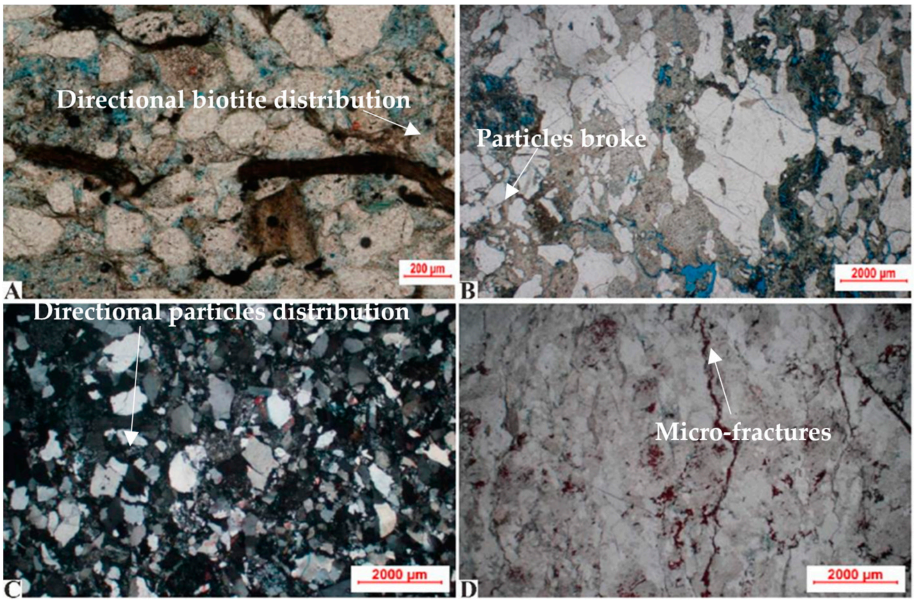

Figure 5. Thin-section photos of mechanical compaction of sandstone reservoir in steep slope zone of Lufeng Sag: (**A**) Well LF X-D, En-3 member, 3642.0 m, has a directional biotite distribution and extrusion deformation; (**B**) Well LF X-A, 3877.0 m, Wen-1 and 2 member, showed a large amount of pseudo-matrix, and clay minerals among the particles, poor sorting of clastic particles, and a large number of particles broke; (**C**) Well LF X-C, 3614.5 m, En-3 member has directional arrangement of particles, poor overall pore development; (**D**) Well LF X-C, 3734.0 m, prepaleogene, granite developed a large number of micro-fractures under strong compaction.

Thin-section identification and whole-rock XRD analysis show that the cementation of sandstone reservoirs in the study area is mainly siliceous, argillaceous, and carbonatic, and cement content is generally not high (Figure 6). However, it has a significant influence on the petrophysical characteristics of the reservoir. The siliceous cement in the study area is mainly characterized by secondary enlargement of quartz, and the enlarged quartz particles are in concave and convex contact and closely arranged. What is more, idiomorphic quartz crystals can also be observed, and the degree of idiomorphism is high. In addition, clay-mineral cementation is generally developed in the study area, and the argillaceous cement is heterogeneous and unevenly distributed, and sericitization occurs. The clay cement developed in the pores will block the throat and reduce the porosity and permeability of the reservoir. Common clay minerals in the Wenchang–Enping Formation sandstone reservoir include illite, montmorillonite, kaolinite, and chlorite. Finally, carbonate cement was mainly developed in the late period, with calcite and iron calcite as the main components and a small amount of iron dolomite. The calcite cements were stained dark red, and dolomite cements were stained dark blue with high iron content, with abundant cements indicating the diagenetic fluid had a strong transformation effect. All of the carbonate cement is amorphous, filling the original feldspar and debris dissolution pores while being partly associated with clay minerals such as kaolinite. In addition, a small amount of siderite developed here (Figure 7).

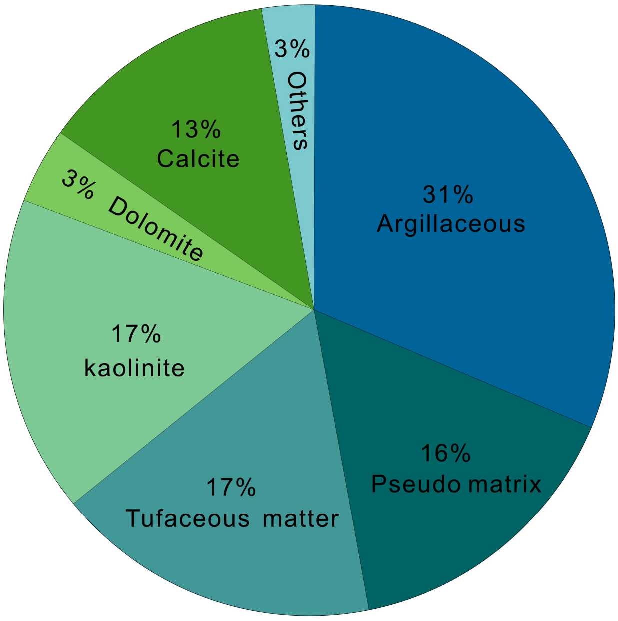

Figure 6. Pie chart of the proportion of main cement in sandstone reservoir in steep slope zone of Lufeng Sag.

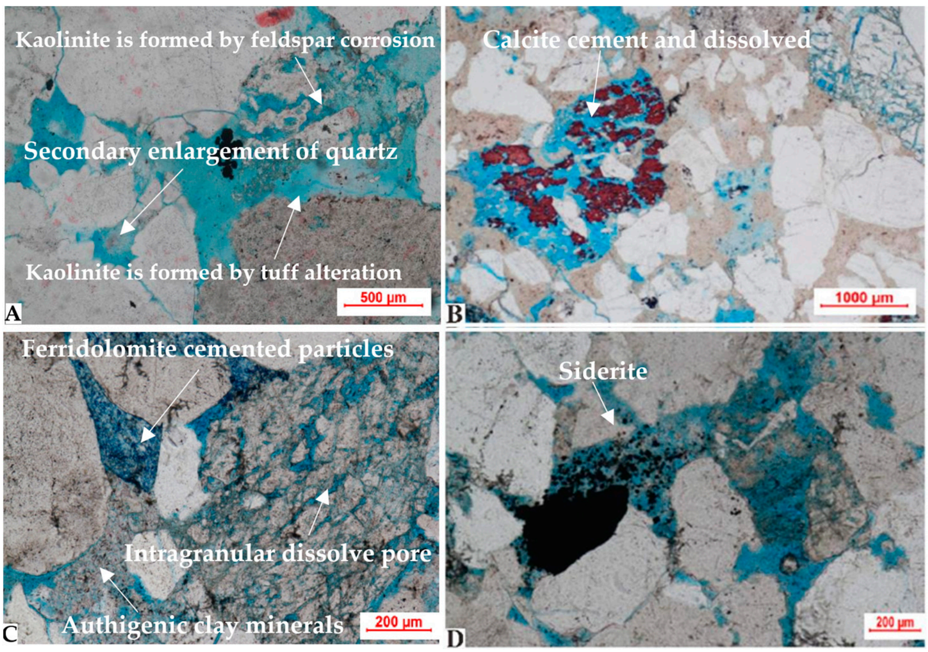

Figure 7. Thin-section photos of calcareous cementation, argillous cementation, and carbonate cementation of sandstone reservoir in steep slope zone of Lufeng Sag: (**A**) Well LF X-C, En-1 and 2 member, 3596 m, secondary enlargement of quartz is shown in the left, and the kaolinite is formed by tuff alteration and feldspar corrosion in the right; (**B**) Well LF X-B, 3879.2 m, Prepaleogene, feldspathic particles were replaced by calcite in the early stage, and the feldspathic part strongly dissolved, leaving only a large amount of calcite; (**C**) Well HZ Z-A, 3256.2 m, En-2 member, cemented iron-dolomite particles were produced, and authigenic clay minerals such as kaolinite were deposited

in situ or filled between grains; (**D**) Well HZ Z-A, 3260.8 m, Wen-1 and 2 member, on the left, a small amount of ferridolomite cemented particles are produced, and feldspar dissolves to form intragranular dissolve pore; on the right, authigenic clay minerals such as kaolinite are formed and filled between grains.

The deep reservoirs can be significantly improved by dissolution, which is called additive diagenesis. The atmospheric fresh water and the acidic fluid produced during the maturation of organic matter can promote dissolution development [19,20]. Through the image analysis of the thin sections, the dissolution phenomenon is generally developed in the study area, which mainly occurs in the inner, cleavage, and interparticle of the particles (Figure 8). The most commonly dissolved mineral is feldspar, and the dissolution of quartz and calcite cement is rare, with crystal shapes remaining intact and edges remaining relatively regular, indicating minimal signs of dissolution. However, occasional dissolution of clay matrix can be observed, leading to a limited number of dissolution micro-cracks and intergranular pores. These features provide insights into the reservoir's petrophysical properties and the potential for fluid flow and storage within the formation.

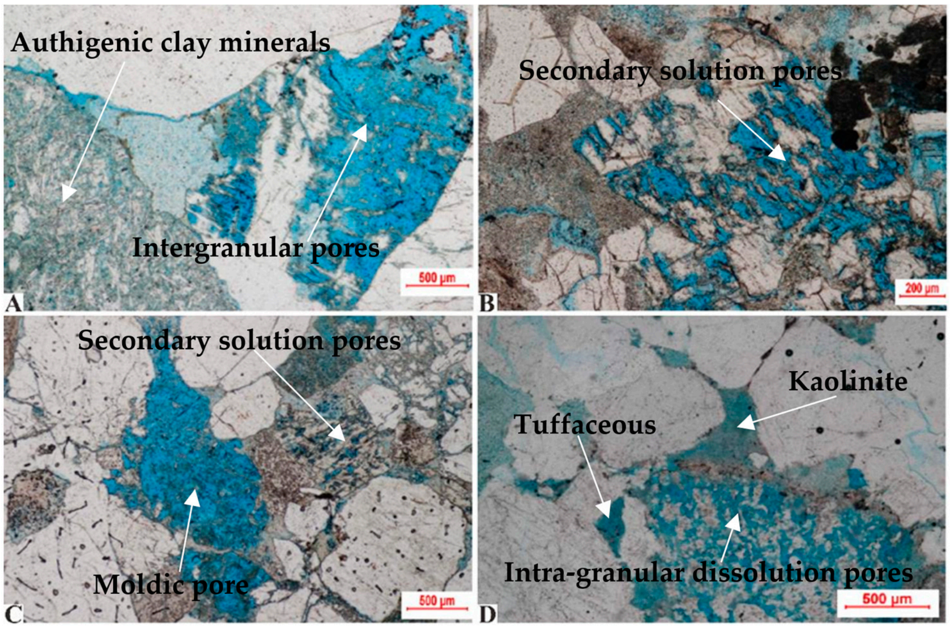

Figure 8. Thin section photo of sandstone reservoir dissolution in steep slope zone of Lufeng Sag: (**A**) Well LF X-D, 3593.0 m, En-3 member, only little remains of feldspar dissolution, authigenic kaolinite filling the intergranular and intergranular pores can be observed; (**B**) Well LF X-A, 3872 m, Wen-1-2 member, some feldspar dissolved strongly to form secondary dissolution pores, and a large number of pseudo-matrix filling grains; (**C**) Well LF X-A, 3878.0 m, Wen-1-2 member, feldspar partially dissolved to form secondary dissolution pores, or completely dissolved to form moldic pore; (**D**) Well LF X-C, 3538.0 m, En-3 member, the intergrain is filled with clay-like tuffaceous matter, and kaolinite formed by particle dissolution such as feldspar is present, and a large number of particles such as feldspar are dissolved, forming a small number of intra-granular dissolution pores.

According to the pore evolution and dissolution zonation and petrophysical properties of sandstone reservoirs in the steep slope zone of Lufeng Sag (Figure 9), there are mainly two stages of secondary pore-development zones, and the distribution is as follows. The first-order secondary dissolution pore development zone located at a buried depth of 3300–3500 m, only develops in the Wen-4 member of the northwest steep slope zone of Lufeng 13 subsag, which is dominated by the mixed dissolution of formation water and acidic organic water discharged by decarboxylate [19] and has good characteristics of pore and seepage development [20]. The second-order secondary dissolution pore-development zone located at the buried depth of 3600–3800 m only developed in the En-4 member of the

LF X transition zone in Lufeng Sag was dominated by the dissolution of acidic organic water discharged by decarboxylate [19]. Although the primary pores and remaining intergranular pores in the dissolution zone have been significantly reduced compared to those in the first-order dissolution zone due to further compaction and filling and cementation in the process of burial enhancement, many secondary pores can be generated mainly because the dissolution zone is closer to the source rock and more susceptible to acidic fluid transformation. Therefore, the reservoir still has higher porosity, a more comprehensive distribution range, and stronger dissolution strength than the first-order dissolution zone.

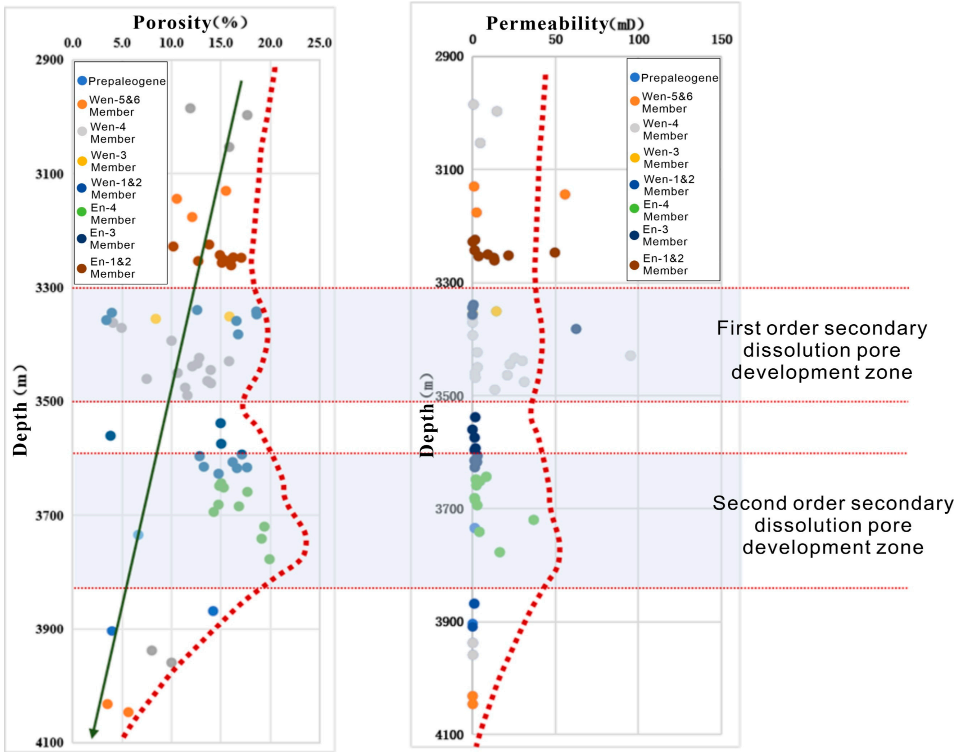

Figure 9. Distribution characteristics of dissolution pore development zone of seven wells in steep slope zone of Lufeng Sag.

4.3. Development Mechanism and Distribution Characteristics of Sweet Spot Reservoir

4.3.1. Controlling Factors of Reservoir's Petrophysical Property

Taking well LF X-A as an example, comparing the influences of sedimentary facies types and single-sand body thickness on reservoir petrophysical properties between the Wenchang Formation and Enping Formation, it can be seen that the control effect of sedimentary facies on reservoir petrophysical properties is mainly reflected in sedimentary subfacies and single-sand body thickness (Figure 10). As can be seen from the figure, the petrophysical properties of sandstone reservoirs of the Enping Formation and Wenchang Formation are considerably different. The petrophysical properties of the Enping Formation sandstone reservoirs are significantly superior to those of the Wenchang Formation. The distributary channel in the inner fan delta plain of the Enping Formation has the best reservoir petrophysical property. Meanwhile, the thicker the sand body of the single-layer distributary channel, the higher the permeability of the sandstone reservoir and the better the reservoir's petrophysical property. The Wenchang Formation also has the same rule, and the porosity of the Wenchang Formation sandstone reservoir is also greatly affected by the thickness of a single-sand body, while the Enping Formation is only related to permeability.

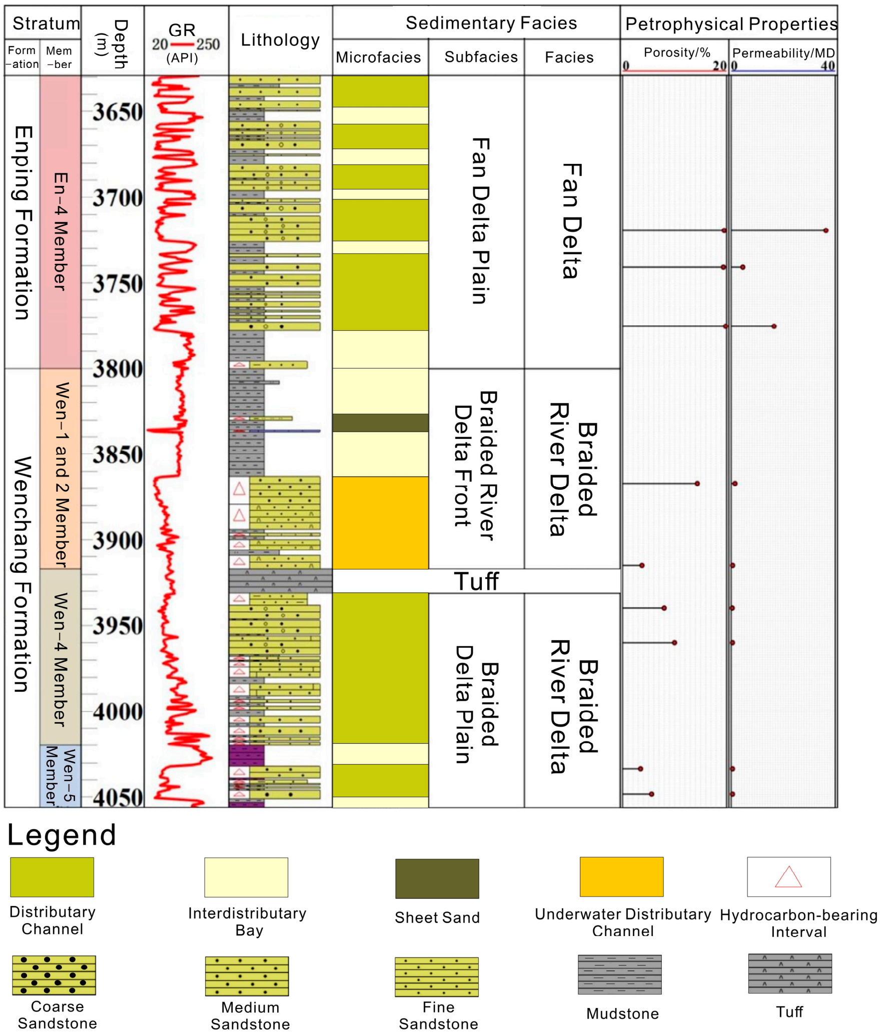

Figure 10. Comprehensive column diagram of sedimentary microfacies and reservoir petrophysical properties of well LF X-A in steep slope zone of Lufeng Sag.

Taking well LF X-D as an example, a consistent rule can be obtained by comparing the influence of different sedimentary microfacies types and single-sand body thickness on reservoir petrophysical properties in the fan delta and braided river delta in the Wechang Formation and Enping Formation. Table 2 shows that the reservoir petrophysical properties of the braided river delta are significantly higher than those of the fan delta, and the petrophysical properties of the fan delta front are significantly higher than those of the fan delta plain. Therefore, the influence of sedimentary facies on the petrophysical properties of the sandstone reservoir is mainly in sedimentary subfacies and single-sand body thickness.

Table 2. Correspondence between sedimentary subfacies and reservoir petrophysical properties of well LF X-D in steep slope zone of Lufeng Sag.

Enping Formation and Wenchang Formation	Average Porosity/%	Mean Permeability/mD
Braided river delta (*n* = 5)	16	31.3
Fan delta (*n* = 15)	6.9	0.33
Braided river delta plain	/	/
Braided river delta front (*n* = 5)	16	31.3
Fan delta plain (*n* = 14)	6.5	0.2
Fan delta front (*n* = 1)	13.1	2.23

The influence of parent rock lithology and transport distance on reservoir petrophysical properties in the steep slope zone of Lufeng Sag is complex. It is necessary to distinguish between different types of parent rock areas and background mechanical compaction. Under weak compaction, the high content of feldspar promotes secondary dissolution pores, and quartz is usually not easily dissolved, which limits the development scale of reservoir dissolution and is not conducive to improving the reservoir's petrophysical properties. Under strong compaction, the opposite situation is observed. The high quartz content improves the compaction resistance of the reservoir, thus retaining many primary and secondary pores. In contrast, the higher the feldspar content will be converted into a large number of matrixes, thus significantly destroying the pores. In addition, the tuff parent rock content has a strong destructive effect on the sandstone reservoir, as shown in the fact that the residual pores between tuffaceous filling grains and compaction further affect the secondary dissolution pores, thus significantly reducing the porosity and permeability of the sandstone reservoir (Figure 11).

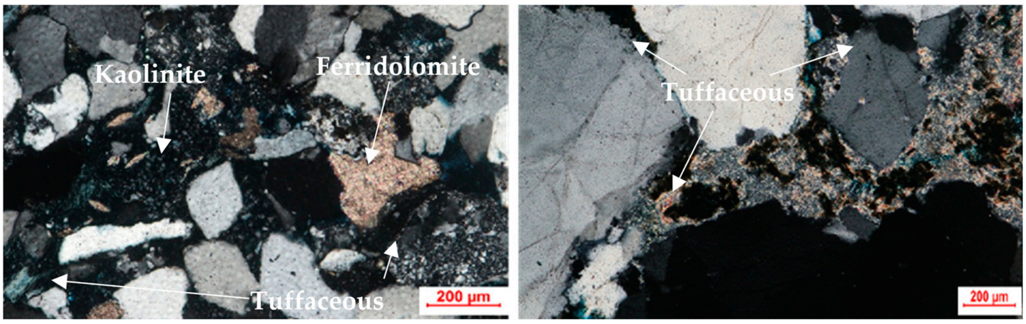

(**A**) (**B**)

Figure 11. Thin section of LF X transition tuffaceous parent rock: (**A**) Well LF X-B, 3339.2 m, En-3 member, tuffaceous is heterobasic, and intergranular pores are filled with authigenic kaolinite and ferridolomite. (**B**) Well LF X-D, 4458.8 m, Wen-3 member, tuffaceous is heterobasic, almost filled with intergranular pores, and only a few dissolution pores exist, showing organic matter infiltration.

4.3.2. Prediction of High-Quality Dissolved Reservoir in Steep Slope Zone

Based on the analysis of the controlling effect of sedimentary facies and parent lithology on the petrophysical properties of sandstone reservoir, the genetic types of high-porosity and low-permeability sandstone reservoir in study area are further defined. Based on the classification criteria of offshore sandstone reservoirs and the effective petrophysical properties of the steep slope zone in Lufeng Sag, it is proposed that sandstone reservoirs with porosity higher than 10% and permeability lower than 1 mD are high-porosity and low-permeability reservoirs. Based on the analysis of the main controlling factors of the sandstone reservoir in the steep slope zone of Lufeng Sag, it is concluded that sedimentary and diagenesis jointly determine the development characteristics of high-porosity and low-permeability reservoirs. However, the main controlling factors of each interval are different due to the evolution of the sedimentary system and mechanical compaction strength. According to the petrophysical properties and thin-section analysis of the Lower Enping Formation of well LF X-C, the reason of low-permeability and high-porosity reservoir is diagenetic fluid retention and precipitation of a large number of clay minerals. In addition, the total amount of clay minerals in Lower Enping Formation of the LF X transition zone also has an excellent negative correlation with porosity, indicating that the content of authigenic clay minerals is the main controlling factor for reservoir porosity reduction (Figure 12).

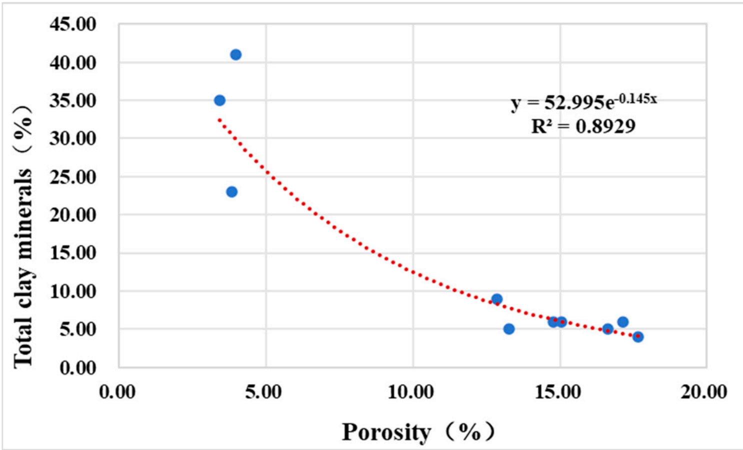

Figure 12. Scatter diagram of correlation between clay mineral content and porosity of sandstone reservoir in the Lower Enping Formation of the LF X transition zone.

Secondary dissolution is the most crucial factor in improving the petrophysical properties of the sandstone reservoir and increasing porosity and permeability in the steep slope zone of Lufeng Sag. Based on the analysis of the main controlling factors of sandstone reservoirs and the genetic analysis of high-porosity and low-permeability reservoirs in the Lower Enping Formation and the Wenchang Formation, the leading causes of secondary dissolution pore development zone of 3600 to 3800 m in the En-4 member of the LF X transition zone are further identified, which lays a good foundation for the prediction of the high-quality sweet-spot reservoir. At the microscopic level, thin-section analysis shows that low clay mineral content is the main reason for the effective preservation of dissolution pores (Figure 13), and the content of clay minerals (such as kaolinite) mainly depends on whether diagenetic fluid can be retained. Therefore, burial depth is not a decisive factor, but the most critical control factor for the development and preservation of secondary dissolution pores is the continuous transformation of feldspar by acidic fluid and the effective discharge of diagenetic fluid

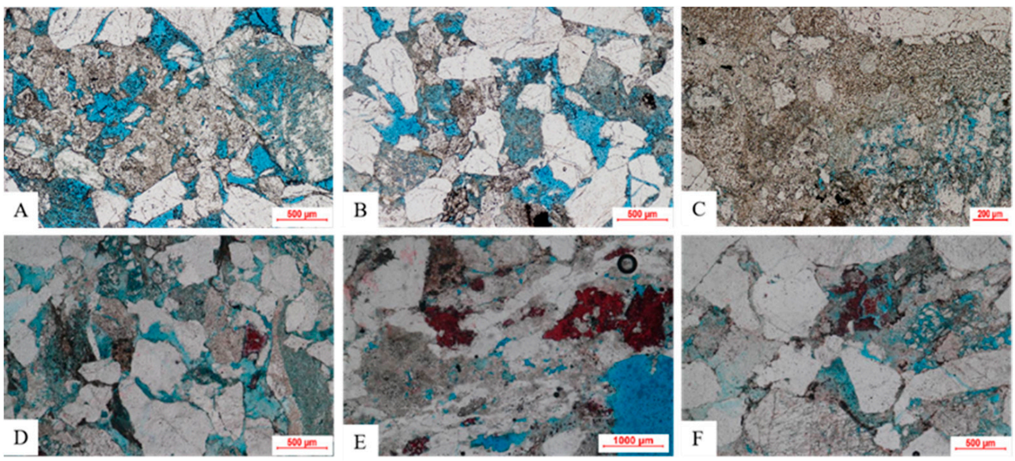

Figure 13. Thin section of reservoir in the LF X transfer zone after being modified by acid fluid: (**A**) Well LF X-A, 3719.6 m, En-4 member, feldspar dissolved to form a secondary solution hole with less interstitials; (**B**) Well LF X-A, 3740.8 m, En-4 member, feldspar dissolved to form a secondary solution hole with less interstitials; (**C**) Well LF X-A, 3867.8 m, Wen-1 and 2 member, feldspar dissolution leads to the formation of kaolinite, which fills the spaces between grains.; (**D**) Well LF X-C, 3614.5 m, En-3 member, feldspar dissolved to form a secondary solution hole filled with in situ retained kaolinite; (**E**) Well LF X-C, 3651.0 m, En-4 member, feldspar dissolved, and iron calcite filled some pores; (**F**) Well LF X-C, 3693.8 m, En-4 member, feldspar dissolution, iron calcite, and kaolinite-filling grain.

5. Discussion

5.1. Effect of Organic-Inorganic Acid Fluid on Sweet Spot Reservoir

The 60 homogenization temperature data of saline fluid inclusions of two wells in the transition zone of Lufeng Sag was analyzed using the homogenization temperature-burial-point method (Figure 14). Based on the data of stratification, interface age, log lithology and Ro, the sedimentary and burial history and thermal history map were made. The uniform temperature distribution interval of saline inclusions associated with hydrocarbon inclusions was projected onto the sedimentary and burial history and thermal history map to obtain the corresponding charging time of hydrocarbon inclusions. As shown in Figure 14, the oil and gas-charging stages of the Wenchang–Enping Formation in the steep slope zone of Lufeng Sag is relatively late, and the accumulation time corresponding to the homogenization temperature of associated brine inclusions is 5-0 Ma. However, the CO_2 charging time was earlier, mainly from 35 to 40 Ma. Therefore, the reservoir was reformed by acidic fluid before oil and gas charging. In addition, most scholars believe that releasing organic–inorganic acids from the thermal evolution of organic matter is an essential reason for forming secondary pores in the diagenesis of clastic rock reservoirs [35–41]. Due to the development of primary pores in the southern part of Lufeng Sag, the Eocene reservoir has a good pore structure, which is conducive to the entry of acidic fluids into the reservoir and the removal of dissolved products, forming more clean and unfilled dissolution pores and improving the porosity and permeability of the reservoir.

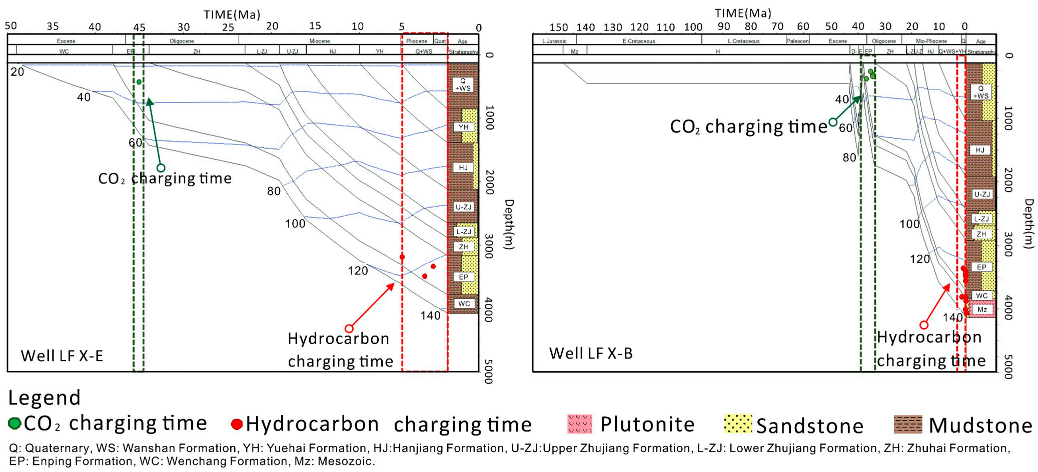

Figure 14. Burial history and fluid-charging time of Wells LF X-E and LF X-B in transition zone of Lufeng Sag, the difference of the sedimentary and burial history and thermal history map between the two wells is due to their location in the LF-X transition zone, where the tectonic activity is very complex.

Developing a secondary dissolution zone in the fan delta sand body is significantly related to its development location. The fan delta front preferentially receives the transformation of organic–inorganic acidic fluids, and more dissolution zones are developed. In contrast, the near margin of the fan delta is more prone to fluid retention, and the diagenetic facies of the developed fan delta are dominated by authigenic minerals (Figure 13). In addition, by comparing the diagenetic facies distribution characteristics of the braided river delta sandstone reservoirs in well HZ Z-A and well LF X-A, it can be seen that the braided river delta sand body is relatively more complex. Due to its better petrophysical characteristics, the fluid has relatively better mobility, so its near-end thick sandstone usually accepts fluid transformation. Therefore, the development of a secondary dissolution zone in the braided river delta sand body is related to the location of reservoir development and the thickness of sand body development (Figure 15). There are the following favourable positions for dissolution facies in braided river delta: first, the end part of the thin layer is preferentially reformed by diagenetic fluid, more dissolution zones are developed, and diagenetic fluid is easy to migrate to other locations, which can effectively avoid the risk of fluid retention and precipitation; secondly, because the sand layer is thicker, the diagenetic mineral precipitation is less, which can promote the development of the dissolution zone.

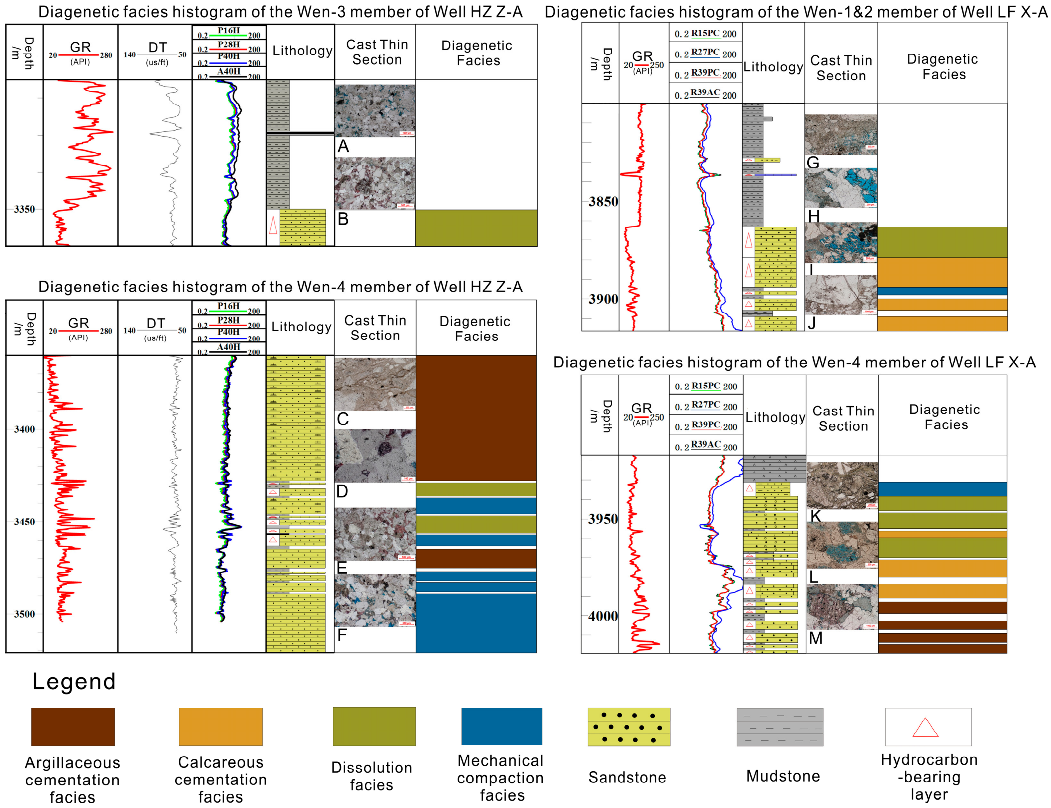

Figure 15. Diagenetic facies distribution characteristics of braided river delta in steep slope zone of Lufeng Sag: (**A**) Well HZ Z-A, 3350 m, Wen-3 member, is mainly medium-grained, and some feldspar and cuttings form intra-granular dissolution pores; (**B**) Well HZ Z-A, 3354.7 m, Wen-3 member, mainly medium grain, a small amount of mud, kaolinite is produced in scaly form; (**C**) Well HZ Z-A, 3361.7 m, Wen-4 member, the mud is generally developed and filled between grains in a heterobasic or striped shape; (**D**) Well HZ Z-A, 3370.62 m, Wen-4 member, the sorting of detrital particles was poor, and some quartz secondary increased; (**E**) Well HZ Z-A, 3393.26 m, Wen-4 member, the kaolinite is scaly and the pores are moderately developed; (**F**) 3454.7 m, medium-grained, coarse-grained followed, kaolinite is scaly, pyrite is coagulated block; (**G**) Well LF X-A, 3867.80 m, Wen-1 and 2 member, a large amount of pseudo-matrix debris, kaolinite filled with intergranular pores; (**H**) Well LF X-A, 3869.00 m, Wen-1 and 2 member, a large amount of pseudo-matrix debris was formed, and the intergranular pores were filled with kaolinite; (**I**) Well LF X-A, 3872 m, Wen-1 and 2 Member, a large amount of pseudo-matrix; (**J**) Well LF X-A, 3909.3 m, Wen-1 and 2 member, calcite filled pores; (**K**) Well LF X-A, 3923.3 m, Wen-4 member, the mud is generally developed, and it is filled between grains in a heterobasic shape; (**L**) Well LF X-A, 3938 m, Wen-4 member, some of the feldspar debris dissolved to form secondary solution pores, and some of the interstitial materials became pseudo-matrix; (**M**) Well LF X-A, 4011.7 m, Wen-4 member, iron calcite cement, kaolinite is scaly.

5.2. Prediction of Eocene Favorable Area of Steep Slope Zone in Lufeng Sag

Previous studies have confirmed that the geochemical characteristics of oil and gas in the steep slope zone of the Lufeng Depression have a strong consistency with the mudstone of the Wenchang Formation, indicating that the oil and gas have near-source-charging characteristics [42]. Most of the oil and gas found in the steep slope zone of Lufeng Sag are closely related to faults, and the late active faults control the migration and accumulation of oil and gas, a relatively crucial vertical transport path. Based on the combination of reservoir-cap assemblages, hydrocarbon generation and expulsion times, fault activity, and hydrocarbon accumulation periods in the steep slope zone of Lufeng Sag, the event map of the Wenchang–Enping Formation hydrocarbon system in the steep slope zone of Lufeng Sag is drawn. The critical moments of the two periods are summarized as follows: 1. The first phase corresponds to the T60–T40 sedimentary period (23.03–15.97 Ma), which is the trap of the steep slope zone, and the primary generation and hydrocarbon expulsion period began. 2. The second phase corresponds to the sedimentary period from T32 to the Quaternary system, about 5 Ma till now, and it is mainly characterized by continuous accumulation characteristics and average accumulation temperature reflected by fluid inclusions. The event map of the Wenchang–Enping Formation hydrocarbon system in Lufeng Sag shows that the Wenchang–Enping Formation reservoir–cap combination is well matched, and the fault activity controlling vertical hydrocarbon migration from mudstone from the Lower Wenchang Formation to the braided river delta sandstone reservoir of the Enping Formation in the steep slope zone is enhanced, which is well matched with hydrocarbon generation and expulsion time. (Figure 16).

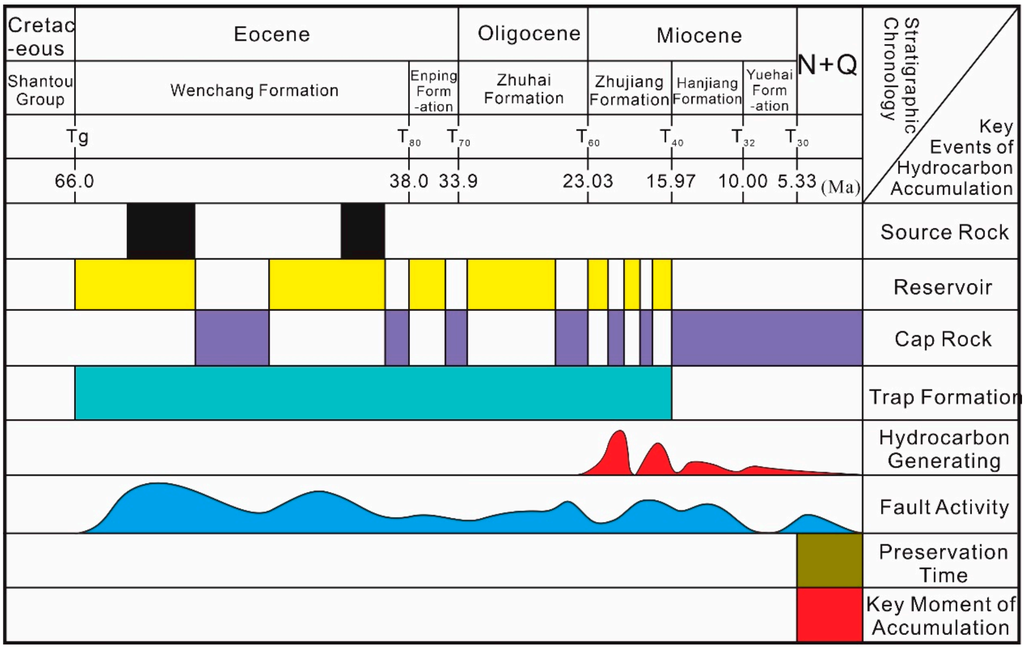

Figure 16. Hydrocarbon accumulation event diagram of Wenchang-Enping Formation in steep slope zone of Lufeng Sag.

Considering the influence of high-quality sweet-spot reservoirs and fault activity on oil and gas migration and accumulation, the favourable zones in different regions of Lufeng Sag are selected, and different accumulation models are established.

The deep layer of the LF Y area has the following advantages for accumulation. First, the favourable area is located near the fault, and the deep section ridge is developed. Second, the sandstone reservoirs of the fan delta in the Wen-4 member has a large contact area with the lacustrine mudstone of the Wen-5 and 6 member. Finally, the favourable area is located in the acidic fluid priority transformation area, which can effectively avoid fluid retention and precipitation (Figure 17).

The fan-delta front of the Wen-3 member in the LF X area has the following advantages. Firstly, it has multi-layer and multi-type reservoir distribution (buried-hill, Mesozoic, Paleogene, Neogene). Second, the Paleogene faults are well matched, and the large-scale sand bodies are developed. Thirdly, a relatively longer transport distance can reduce tuff and argillaceous content. Fourth, diagenetic fluid first dissolves the reservoir material in the front of the fan delta and carries it to the plain. Fifthly, the up-dip direction of the mudstone near the middle and deep lake points to the fan delta front of Wen-3 member.

Sixth, the thick mudstone overlying the sandstone in front of the fan delta is a good cover layer (Figure 18).

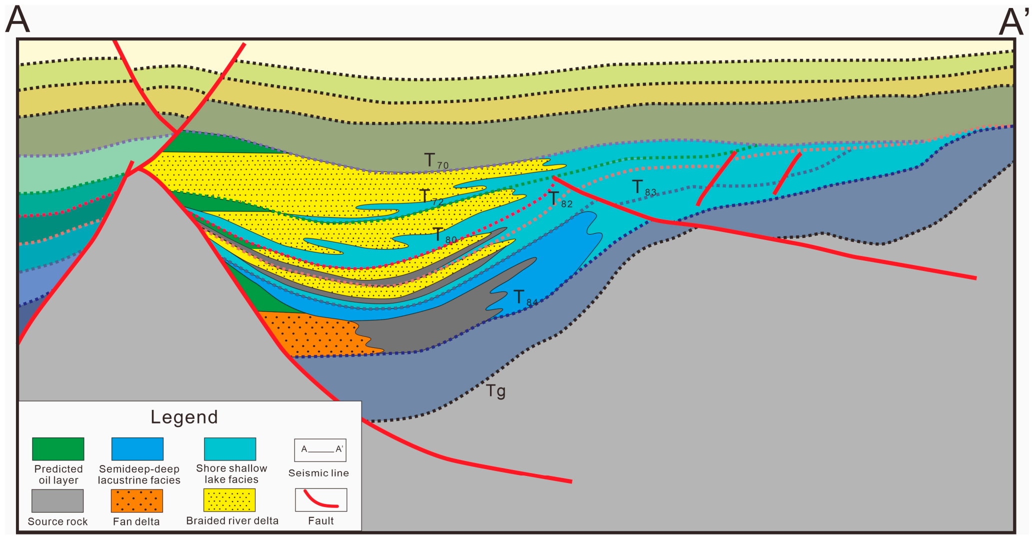

Figure 17. Deep Eocene petroleum accumulation model of the near end of thick braided river deltas and fan deltas in LF Y area.

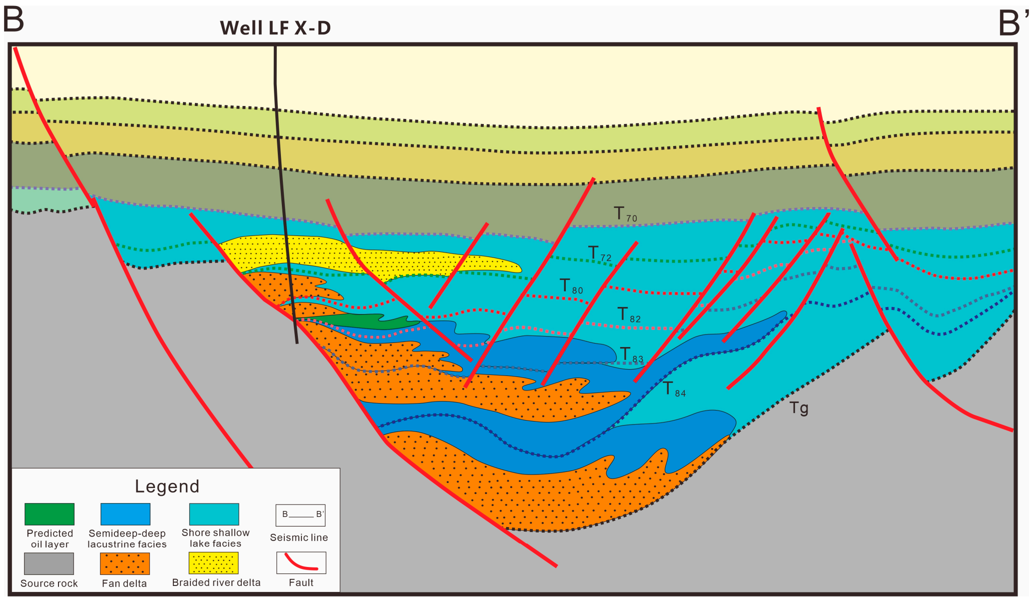

Figure 18. Deep Eocece petroleum accumulation model in the front of thin fan delta near Well LF X-D in LF X area.

6. Conclusions

(1) Parent rock type and transport distance, parent rock properties, tuffaceous content, sand body connectivity, diagenetic fluid retention, and single-sand body thickness jointly control reservoir-development characteristics in the steep slope zone of the Lufeng Sag in the Pearl River Mouth Basin. Although the compaction background is generally developed in the Paleogene of Lufeng Sag, continuous transformation and effective discharge of acidic fluid is an important controlling factor for developing secondary dissolution pore zones in high-quality reservoir segments.

(2) Through the analysis of 1140 thin sections from 57 depth points, five types of diagenesis are identified in the Lufeng Sag. Combined with the control factors of the secondary dissolution pore-development zone and the vertical and plane distribution

characteristics of diagenetic facies in the steep slope zone of Lufeng Sag, it is finally determined that the front edge of the fan delta, the front of the thin layer, and the near margin of the thick layer of the braided river delta are favourable zones for the development of the high-quality sweet-spot reservoir.

(3) The oil and gas charging time of the Wenchang–Enping Formation in the steep slope zone of the Lufeng Depression is relatively late, and only the first phase of 5-0 ma oil and gas charging has been found. However, the CO_2 charging time in the steep slope zone is earlier, mainly between 35–40 MA. As a result, the reservoir has been modified by an inorganic-organic acidic fluid before oil and gas charging. According to the analysis of the critical moments of hydrocarbon accumulation and the dominant sedimentary facies zones, it is concluded that the fan delta front of well LF X-D and the deep layer of LF Y may have better conditions for hydrocarbon accumulation and preservation, which is a favourable area for the development of the steep slope zone in the Lufeng Depression.

Author Contributions: K.Z.: Validation; Supervision; Project administration; Funding acquisition; L.B.: Methodology; Software; Formal analysis; Investigation; Writing-original draft; S.Z.: Methodology; Software; Investigation; Data curation; Writing-review and editing; K.F.: Methodology; Data curation; Project administration. All authors have read and agreed to the published version of the manuscript.

Funding: This study was Supported by the National Natural Science Foundation of China (No. 92055203).

Data Availability Statement: Data will be made available on request.

Acknowledgments: We appreciate the valuable suggestions provided by the editor and anonymous reviewers regarding our manuscript.

Conflicts of Interest: The authors declare no conflict of interest.

References

1. He, D.; Jia, C.; Zhao, W.; Xu, F.; Luo, X.; Liu, W.; Tang, Y.; Gao, S.; Zheng, X.; Li, D.; et al. Research progress and key issues of ultra-deep oil and gas exploration in China. *Petro. Explor. Dev.* **2023**, *50*, 1333–1344. [CrossRef]
2. Laubach, S.E.; Zeng, L.; Hooker, J.N.; Wang, Q.; Zhang, R.; Wang, J.; Ren, B. Deep and ultra-deep basin brittle deformation with focus on China. *J. Struct. Geol.* **2023**, *175*, 104938. [CrossRef]
3. Wang, P.; Wang, G.; Chen, Y.M.; Hao, F.; Yang, X.; Hu, F.; Zhou, L.-L.; Yi, Y.; Yang, G.; Wang, X.; et al. Formation and preservation of ultra-deep high-quality dolomite reservoirs under the coupling of sedimentation and diagenesis in the central Tarim Basin, NW China. *Mar. Pet. Geol.* **2022**, *149*, 106084. [CrossRef]
4. Dutton, S.P.; Loucks, R.G. Diagenetic controls on evolution of porosity and permeability in lower Tertiary Wilcox sandstones from shallow to ultradeep (200–6700 m) burial, Gulf of Mexico Basin, U.S.A. *Mar. Pet. Geol.* **2010**, *27*, 69–81. [CrossRef]
5. Bloch, S.; Lander, R.H.; Bonnell, L. Anomalously High Porosity and Permeability in Deeply Buried Sandstone Reservoirs: Origin and Predictability. *AAPG Bull.* **2002**, *86*, 301–328.
6. Pang, X.; Jia, C.; Zhang, K.; Li, M.; Chen, J. The dead line for oil and gas and implication for fossil resource prediction. *Earth Syst. Sci. Data* **2020**, *12*, 577–590. [CrossRef]
7. Jia, C.; Pang, X. Research processes and main development directions of deep hydrocarbon geological theories. *Acta Petrol. Sin.* **2015**, *36*, 1457–1469. (In Chinese with English Abstract)
8. Yang, L.; Zhaojie, X.; Zhe, C.; Haijun, J.; Ruyue, W. Progress and development directions of deep oil and gas exploration and development in China. *China Pet. Explor.* **2019**, *25*, 45–57. (In Chinese with English Abstract)
9. Aase, N.E.; Walderhaug, O. The effect of hydrocarbons on quartz cementation: Diagenesis in the Upper Jurassic sandstones of the Miller Field, North Sea, revisited. *Petrol. Geosci.* **2005**, *11*, 215–223. [CrossRef]
10. Cao, Y.; Yuan, G.; Li, X.; Wang, Y.; Xi, K.; Wang, X.; Jia, Z.; Yang, T. Characteristics and origin of abnormally high porosity zones in buried Paleogene clastic reservoirs in the Shengtuo area, Dongying Sag, East China. *Petrol. Sci.* **2014**, *11*, 346–362. [CrossRef]
11. Zeng, Q.; Mo, T.; Jilong, Z.; Tang, Y.; Zhang, R.; Xia, J.; Hu, C.; Shi, L.-h. Characteristics, genetic mechanism and oil & gas exploration significance of high-quality sandstone reservoirs deeper than 7000 m: A case study of the Bashijiqike Formation of Lower Cretaceous in the Kuqa Depression, NW China. *Nat. Gas Ind. B.* **2020**, *7*, 317–327. (In Chinese with English Abstract)
12. Shi, H. On heterogeneous distribution and differential enrichment by zones of hydrocarbon resources:a case in Zhu I depression, Pearl River Mouth basin. *China Offshore Oil Gas* **2013**, *25*, 1–8+25+93. (In Chinese with English Abstract)

13. Shi, H.; Zhu, J.; Jiang, Z.; Shu, Y.; Xie, T.; Wu, J. Hydrocarbon resources reassessment in Zhu I depression, Pearl River Mouth basin. *China Offshore Oil Gas* **2009**, *21*, 9–14. (In Chinese with English Abstract)
14. Yu, F.; Koyi, H.A.; Zhang, X. Intersection patterns of normal faults in the Lufeng Sag of Pearl River Mouth Basin, China: Insights from 4D physical simulations. *J. Struct. Geol.* **2016**, *93*, 67–90. [CrossRef]
15. Chen, S.; Xu, S.; Cai, Y.; Ma, X. Wrench related faults and their control on the tectonics and Eocene sedimentation in the L13–L15 sub-sag area, Pearl River Mouth basin, China. *Mar. Pet. Geol.* **2018**, *39*, 363–381. [CrossRef]
16. Ma, B.; Qi, J.; Chen, W.; Zhao, M. Fault interaction and evolution during two-phase rifting in the Xijiang Sag, Pearl River Mouth Basin, northern South China Sea. *Geol. J.* **2019**, *55*, 1128–1147. [CrossRef]
17. Ye, Q.; Mei, L.; Shi, H.; Shu, Y.; Camanni, G.; Wu, J. A low-angle normal fault and basement structures within the Enping Sag, Pearl River Mouth Basin: Insights into late Mesozoic to early Cenozoic tectonic evolution of the South China Sea area. *Tectonophysics* **2018**, *731*, 1–16. [CrossRef]
18. Ge, J.; Zhu, X.; Zhao, X.; Liao, J.-j.; Ma, B.; Jones, B.G. Tectono-sedimentary signature of the second rift phase in multiphase rifts: A case study in the Lufeng Sag (38–33.9 Ma), Pearl River Mouth Basin, south China sea. *Mar. Pet. Geol.* **2010**, *114*, 104218. [CrossRef]
19. Zhu, X.; Ge, J.; Wu, C.; Zhang, X.; Wang, X.; Li, X.; Li, M. Reservoir characteristics and main controlling factors of deep sandstone in Lufeng sag, Pearl River Mouth Basin. *Acta Petrol. Sin.* **2019**, *40*, 69–80. (In Chinese with English Abstract)
20. Surdam, R.C.; Crossey, L.J.; Hagen, E.S.; Heasler, H.P. Organic-Inorganic Interactions and Sandstone Diagenesis. *AAPG Bull.* **1989**, *73*, 1–23.
21. Zhang, X.; Wang, X.; Shu, Y.; Zhang, S.; Wang, Y. Geological characteristics and forming conditions of large and medium oilfields in Lufeng Sag of Eastern Pearl River Mouth Basin. *J. Cent. South Univ. Nat Sci Ed.* **2017**, *48*, 2979–2989. (In Chinese with English Abstract)
22. Wang, X.; Zhang, X.; He, M.; Zhang, S.; Wuchen, B. Characteristics and controlling factors of reservoir development in the Wenchang Formation, Southern Lufeng Sag, Pearl River Mouth Basin. *Oil Gas Geol.* **2017**, *38*, 1147–1155. (In Chinese with English Abstract)
23. Zhu, W.; Cui, H.; Wu, P.; Sun, H. New development and outlook for oil and gas exploration in passive continental margin basins. *Acta Petrol. Sin.* **2017**, *38*, 1099–1109. (In Chinese with English Abstract)
24. Zhang, X.; Liu, P.; Wang, W. Controlling Effect of Tectonic Transformation in Paleogene Wenchang Formation on Oil and Gas Accumulation in Zhu I Depression. *Earth Sci.* **2021**, *46*, 1797–1813. (In Chinese with English Abstract)
25. Gao, Y.; Wang, X.; Lin, H.; Que, X.; Xiao, Z.; Jia, L. Characteristics and significances of the tectono-sedimentary transitional unconformity in Enping Formation of Lufeng Sag, Pearl River Mouth Basin. *Nat. Gas Geosci.* **2021**, *32*, 961–970. (In Chinese with English Abstract)
26. Dai, Y.; Niu, Z.; Wang, X.; Wang, X.; Xiao, Z.; Zhang, K.; Zhao, X. Differences of hydrocarbon enrichment regularities and their main controlling factors between Paleogene and Neogene in Lufeng Sag, Pearl River Mouth Basin. *Acta Petrol. Sin.* **2019**, *40*, 41–52. (In Chinese with English Abstract)
27. Zhu, D.; Zhang, X.; Lei, Y.; Qiu, X.; Yang, Y. Tectonic characteristics of Lufeng North area and the exploration direction of the Enping Formation. *China Offshore Oil Gas* **2020**, *32*, 44–53. (In Chinese with English Abstract)
28. Wang, H.; Fu, X.; Fan, M.; Wang, S.; Meng, L.; Du, W. Fault growth and linkage: Implications for trap integrity in the Qi'nan area of the Huanghua Depression in Bohai Bay Basin, China. *Mar. Pet. Geol.* **2022**, *145*, 105875. [CrossRef]
29. Cullen, A.; Reemst, P.; Henstra, G.; Gozzard, S.; Ray, A. Rifting of the South China Sea: New perspectives. *Petrol. Geosci.* **2010**, *16*, 273–282. [CrossRef]
30. Yan, Y.; Xia, B.; Lin, G.; Liu, B.; Yan, P.; Li, Z. The sedimentary and tectonic evolution of the basins in the north margin of the South China Sea and geodynamic setting. *Mar. Pet. Geol.* **2005**, *25*, 53.
31. Li, S.; Suo, Y.; Liu, X.; Dai, L.; Yu, S.; Zhao, S.; Ma, Y.; Wang, X.; Cheng, S.; An, H. Basin dynamics and basin groups of the South China Sea. *Mar. Pet. Geol.* **2013**, *32*, 55–78. [CrossRef]
32. Zhong, Z.; Shi, H.; Zhu, M.; Pang, X.; He, M.; Zhao, Z.; Liu, S.; Wang, F. A discussion on the tectonic-stratigraphic framework and its origin mechanism in Pearl River Mouth Basin. *China Offshore Oil Gas.* **2014**, *26*, 20–29. (In Chinese with English Abstract)
33. Wu, Z.; Hu, Y.; Zhi, Z. Cenozoic faults characteristics and regional dynamic background of Panyu 4 subsag, Zhu I Depression. *J. China Univ. Petrol. Nat. Sci. Ed.* **2015**, *39*, 1–9. (In Chinese with English Abstract)
34. Hu, Y.; Wu, Z.; Zhong, Z.; Zhang, J.; Yu, W.; Wang, G.; Liu, Y.; Wang, S. Characterization and genesis of the middle and late Eocene tectonic changes in Zhu 1 depression of Pearl River Mouth basin. *Oil Gas Geol.* **2016**, *37*, 779–785. (In Chinese with English Abstract)
35. Zhu, D.; Meng, Q.; Jin, Z.; Liu, Q.; Hu, W. Formation mechanism of deep Cambrian dolomite reservoirs in the Tarim basin, northwestern China. *Mar. Pet. Geol.* **2015**, *59*, 232–244. [CrossRef]
36. Hao, F.; Zhang, X.; Wang, C.; Li, P.; Guo, T.; Zou, H.; Zhu, Y.; Liu, J.; Cai, Z. The fate of CO_2 derived from thermochemical sulfate reduction (TSR) and effect of TSR on carbonate porosity and permeability, Sichuan Basin, China. *Earth Sci. Rev.* **2015**, *141*, 154–177. [CrossRef]
37. Zhu, G.; Zhang, S.; Liang, Y.; Ma, Y.; Dai, J.; Zhou, G. Dissolution and alteration of the deep carbonate reservoirs by TSR: An important type of deep-buried high-quality carbonate reservoirs in Sichuan basin. *Acta. Petrol. Sin.* **2006**, *22*, 2182–2194. (In Chinese with English Abstract)

38. Zhu, D.; Meng, Q.; Jin, Z.; Hu, W. Fluid environment for preservation of pore spaces in a deep dolomite reservoir. *Geofluids* **2015**, *15*, 527–545. [CrossRef]
39. Jia, L.; Cai, C.; Yang, H.; Li, H.; Wang, T.; Zhang, B.; Jiang, L.; Tao, X.-W. Thermochemical and bacterial sulfate reduction in the Cambrian and Lower Ordovician carbonates in the Tazhong Area, Tarim Basin, NW China: Evidence from fluid inclusions, C, S, and Sr isotopic data. *Geofluids* **2015**, *15*, 421–437. [CrossRef]
40. Jiang, L.; Worden, R.H.; Yang, C. Thermochemical sulphate reduction can improve carbonate petroleum reservoir quality. *Geochim. Cosmochim. Acta.* **2018**, *223*, 127–140. [CrossRef]
41. Lu, Z.; Chen, H.; Qing, H.; Chi, G.; Chen, Q.; You, D.; Yin, H.; Zhang, S. Petrography, fluid inclusion and isotope studies in Ordovician carbonate reservoirs in the Shunnan area, Tarim basin, NW China: Implications for the nature and timing of silicification. *Sediment. Geol.* **2017**, *359*, 29–43. [CrossRef]
42. He, Y.; Lei, Y.; Qiu, X.; Xiao, Z.; Zheng, Y.; Liu, D. Sedimentary paleoenvironment and main controlling factors of organic enrichment in source rocks of the Wenchang Formation in southern Lufeng, Pearl River Mouth Basin. *Earth Sci. Front.* **2024**, *31*, 359–376. (In Chinese with English Abstract)